problem, one can use the computer programs already existing, with very little modification. The theory presented thus unifies all the Green's function theories used for the microstrip structures with any kind of geometry.

REFERENCES

[1] E. Yamashita, "Variational method for the analysis of microstrip like transmission lines," *IEEE Trans. Microwave Theory Tech.*, vol. MTT-16, pp. 251–256, Apr. 1968.

[2] E. Yamashita and K. Atsuki, "Stripline with rectangular outer conductors and three dielectric layers," *IEEE Trans. Microwave Theory Tech.*, vol. MTT-18, pp. 238–244, May 1970.

[3] J. A. Weiss, "Dispersion and field analysis of a microstrip meander line slow-wave structure," *IEEE Trans. Microwave Theory Tech.*, vol. MTT-22, pp. 1194–1201, Dec. 1974.

[4] M. Kobayashi and R. Terakado, "General form of Green's function for multilayer microstrip line with rectangular side walls," *IEEE Trans. Microwave Theory Tech.*, vol. MTT-24, pp. 626–628, 1976.

[5] Y. Chang and I. E. Chang, "Simple method for the variational analysis of a generalized *N*-dielectric layer transmission line," *Electronics Letters*, vol. 6, no. 3, pp. 49–50, Feb. 5, 1970.

[6] R. E. Collin, *Field Theory of Guided Waves*. New York: McGraw-Hill, 1960.

[7] J. Vine, "Impedance networks," in *Field Analysis: Exp. and Comp. Methods*, Vitkovitch, Ed. New York: Van Nostrand, 1966.

Calculation of Electromagnetic Energy Absorption in Prolate Spheroids by the Point Matching Method

R. RUPPIN

Abstract—**The point matching method is used to calculate electromagnetic power absorption in tissue prolate spheroids irradiated by a plane wave. The calculation extends from the low-frequency region and well into the resonance region, but is restricted to spheroids of small eccentricity. A strong dependence of the absorption on the orientation and the polarization of the incident beam is found to occur, in agreement with previous experimental measurements on animals and phantom models.**

I. INTRODUCTION

IN THE THEORETICAL analysis of the interaction of electromagnetic radiation with biological bodies it is usually necessary to resort to simplified geometries. The spherical model has often been used [1]–[3] because of the availability of the Mie theory which provides an analytic solution. Recently, Gandhi [4]–[6] has determined experimentally that there exist interesting polarization effects which cannot be explained by spherical models. An important finding of his measurements was that the resonance absorption for electric polarization (electric field parallel to the long dimension of the irradiated body) was much higher than for the magnetic polarization. The prolate spheroidal model naturally arises as a candidate for the theoretical interpretation of such polarization effects. Unfortunately, this geometry is analytically tractable only in the quasi-static limit, i.e., for wavelengths much longer than the dimensions of the spheroid. A perturbative extension of the low frequency solution has been employed in the calculations of Durney *et al.* [7] and Johnson *et al.* [8]. Their results do exhibit polarization effects, but are still restricted to low frequencies (lower than 30 MHz for man-sized spheroids) and cannot give information about the important resonance region.

In this paper we employ a numerical method to calculate the absorption for higher frequencies, extending well into the resonance region, but only for spheroids with major to minor axis ratio not larger than 1.5. The point matching method used here has been reviewed by Kerker [9], and has more recently been applied to the calculation of the scattering of radio waves from raindrops [10], [11]. In the following section we briefly describe the method, using the notation of Morrison and Cross [11]. The numerical calculations are presented in Section III, and in Section IV the results are discussed and compared with previous experimental results.

II. POINT MATCHING METHOD

We consider a homogeneous prolate spheroid of tissue which is irradiated by an electromagnetic plane wave of frequency ω. Let a denote the length of the semiaxis in the symmetry direction and let b denote the lengths of the other

Manuscript received December 28, 1976; revised April 20, 1977.
The author is with the Soreq Nuclear Research Centre, Yavne, Israel.

0018-9480/78/0200-0087$00.75

two semiaxes. We take the symmetry axis of the spheroid to be along the z axis, and we consider the following three primary polarizations. 1) Magnetic polarization—the magnetic field of the incident wave is parallel to the symmetry axis. 2) Electric polarization—the electric field of the incident wave is parallel to the symmetry axis. 3) Cross polarization—the direction of propagation of the incident wave is parallel to the symmetry axis.

The incident fields are given by

$$\boldsymbol{E}_h^i = \boldsymbol{j} \exp(ik_0 x) \tag{1}$$

$$\boldsymbol{H}_h^i = \frac{k_0}{\omega\mu_0} \boldsymbol{k} \exp(ik_0 x) \tag{2}$$

for the magnetic polarization,

$$\boldsymbol{E}_e^i = -\boldsymbol{k} \exp(ik_0 x) \tag{3}$$

$$\boldsymbol{H}_e^i = \frac{k_0}{\omega\mu_0} \boldsymbol{j} \exp(ik_0 x) \tag{4}$$

for the electric polarization, and

$$\boldsymbol{E}_c^i = \boldsymbol{j} \exp(ik_0 z) \tag{5}$$

$$\boldsymbol{H}_c^i = \frac{k_0}{\omega\mu_0} \boldsymbol{i} \exp(ik_0 z) \tag{6}$$

for the cross polarization. Here $k_0 = \omega(\mu_0 \varepsilon_0)^{1/2}$ and $\boldsymbol{i}, \boldsymbol{j}, \boldsymbol{k}$ are unit vectors along the x, y, z axes, respectively.

The scattered and the transmitted (interior) fields will be expanded in terms of the spherical vector wave functions [12]

$$\boldsymbol{M}_{mn}(\boldsymbol{r}) = \nabla \times (\boldsymbol{r} y_{mn}(\theta,\phi) Z_n(kr)) \tag{7}$$

$$\boldsymbol{N}_{mn}(\boldsymbol{r}) = \frac{1}{k} \nabla \times \boldsymbol{M}_{mn}(\boldsymbol{r}) \tag{8}$$

The radial functions $Z_n(kr)$ are $j_n(k_i r)$ for the transmitted wave and $h_n(k_0 r)$ for the scattered wave, where j_n and h_n are spherical Bessel and Hankel functions, respectively. Here

$$k_i^2 = \omega\mu_0(\omega\varepsilon + i\sigma) \tag{9}$$

where ε and σ are the dielectric constant and the conductivity of the spheroid.

The fields of the scattered wave are expanded in the form

$$\boldsymbol{E}^s = -\sum_{m=-\infty}^{\infty} \sum_{n \geq |m|}{}' (a_{mn} \boldsymbol{M}_{mn} + b_{mn} \boldsymbol{N}_{mn}) \tag{10}$$

$$\boldsymbol{H}^s = \frac{ik_0}{\omega\mu_0} \sum_{m=-\infty}^{\infty} \sum_{n \geq |m|}{}' (a_{mn} \boldsymbol{N}_{mn} + b_{mn} \boldsymbol{M}_{mn}) \tag{11}$$

where the prime denotes that $n = 0$ is excluded from the summation. The fields inside the spheroid are expanded in the form

$$\boldsymbol{E}^t = -\sum_{m=-\infty}^{\infty} \sum_{n \geq |m|}{}' (c_{mn} \boldsymbol{M}_{mn} + d_{mn} \boldsymbol{N}_{mn}) \tag{12}$$

$$\boldsymbol{H}^t = \frac{ik_i}{\omega\mu_0} \sum_{m=-\infty}^{\infty} \sum_{n \geq |m|}{}' (c_{mn} \boldsymbol{N}_{mn} + d_{mn} \boldsymbol{M}_{mn}). \tag{13}$$

The fields given by (10)–(13) satisfy Maxwell's equations in the regions in which they were defined. The incident fields (1)–(6) are expanded in a Fourier series

$$\boldsymbol{E}_q^i = \sum_{m=-\infty}^{\infty} \boldsymbol{e}_{mq}(r,\theta) e^{im\phi} \tag{14}$$

$$\boldsymbol{H}_q^i = \sum_{m=-\infty}^{\infty} \boldsymbol{h}_{mq}(r,\theta) e^{im\phi} \tag{15}$$

where $q = h, e, c$ specifies the polarization (magnetic, electric, or cross). The expansion coefficients for the magnetic and electric polarizations are given by

$$\boldsymbol{e}_{mh}(r,\theta) = \boldsymbol{g}_m(r,\theta) \qquad \boldsymbol{h}_{mh}(r,\theta) = -\frac{k_0}{\omega\mu_0} \boldsymbol{f}_m(r,\theta) \tag{16}$$

$$\boldsymbol{e}_{me}(r,\theta) = \boldsymbol{f}_m(r,\theta) \qquad \boldsymbol{h}_{me}(r,\theta) = \frac{k_0}{\omega\mu_0} \boldsymbol{g}_m(r,\theta) \tag{17}$$

where

$$\boldsymbol{f}_m(r,\theta) = i^m (J_m(k_0 r \sin\theta)(\sin\theta \boldsymbol{i}_\theta - \cos\theta \boldsymbol{i}_r)) \tag{18a}$$

$$\boldsymbol{g}_m(r,\theta) = -i^m \left(\frac{m J_m(k_0 r \sin\theta)}{k_0 r \sin\theta} (\sin\theta \boldsymbol{i}_r + \cos\theta \boldsymbol{i}_\theta) + i J_m'(k_0 r \sin\theta) \boldsymbol{i}_\phi \right) \tag{18b}$$

and J_m is the Bessel function of the first kind of order m. For the cross polarization only the $m = \pm 1$ terms are different from zero, and they are given by

$$\boldsymbol{e}_{\pm 1c}(r,\theta) = \mp \frac{i}{2} e^{ik_0 r \cos\theta} (\sin\theta \boldsymbol{i}_r + \cos\theta \boldsymbol{i}_\theta \pm \boldsymbol{i}_\phi) \tag{19}$$

$$\boldsymbol{h}_{\pm 1c}(r,\theta) = \mp \frac{i}{2} \frac{k_0}{\omega\mu_0} e^{ik_0 r \cos\theta} \cdot (\mp i(\sin\theta \boldsymbol{i}_r + \cos\theta \boldsymbol{i}_\theta) + \boldsymbol{i}_\phi). \tag{20}$$

The coefficients a_{mn}, b_{mn}, c_{mn}, and d_{mn} will be determined from the boundary conditions at $r = R(\theta)$, where $R(\theta)$ defines the surface of the spheroid and is given by the equation

$$R(\theta) = \left(\frac{\sin^2\theta}{b^2} + \frac{\cos^2\theta}{a^2} \right)^{-1/2}. \tag{21}$$

Requiring the tangential components of the electric and the magnetic fields to be continuous we obtain the equations

$$E_\phi^i + E_\phi^s = E_\phi^t \tag{22}$$

$$H_\phi^i + H_\phi^s = H_\phi^t \tag{23}$$

$$E_\theta^i + E_\theta^s + \frac{1}{R}\frac{dR}{d\theta}(E_r^i + E_r^s) = E_\theta^t + \frac{1}{R}\frac{dR}{d\theta} E_r^t \tag{24}$$

$$H_\theta^i + H_\theta^s + \frac{1}{R}\frac{dR}{d\theta}(H_r^i + H_r^s) = H_\theta^t + \frac{1}{R}\frac{dR}{d\theta} H_r^t \tag{25}$$

where all the field components are evaluated at $r = R(\theta)$. Because of the axial symmetry these boundary conditions yield a separate set of equations for each value of m. In the point matching method the summations over n in (10)–(13)

are truncated at $n = N$, say, and for each value of m (up to some large enough M) the boundary conditions (22)–(25) are imposed at $s = N - m + 1 - \delta_{m0}$ points, i.e., at s different values of θ. This yields a system of $4s$ linear equations for the $4s$ coefficients a_{mn}, b_{mn}, c_{mn}, d_{mn}.

After solving the system of linear equations, we can calculate the various cross sections. The extinction cross section is given by [11]

$$\sigma_t = \frac{4\pi}{k_0^2} \operatorname{Re} Q \qquad (26)$$

where, for the magnetic polarization

$$Q = \sum_{m=-\infty}^{\infty} \sum_{n \geq |m|}' (-i)^{n+2} \cdot \left(a_{mn} \frac{dP_n^{|m|}(\cos\alpha)}{d\alpha} + b_{mn} \frac{m}{\sin\alpha} P_n^{|m|}(\cos\alpha) \right) \qquad (27)$$

evaluated at $\alpha = \pi/2$. For the cross polarization Q is given by (27), but evaluated at $\alpha = 0$. For the electric polarization

$$Q = \sum_{m=-\infty}^{\infty} \sum_{n \geq |m|}' (-i)^{n-1} \cdot \left(a_{mn} \frac{m}{\sin\alpha} P_n^{|m|}(\cos\alpha) + b_{mn} \frac{dP_n^{|m|}(\cos\alpha)}{d\alpha} \right) \qquad (28)$$

evaluated at $\alpha = \pi/2$.

The scattering cross section is given by

$$\sigma_s = \frac{4\pi}{k_0^2} \sum_{m=-\infty}^{\infty} \sum_{n \geq |m|}' \frac{n(n+1)(n+|m|)!}{(2n+1)(n-|m|)!} \cdot \left(|a_{mn}|^2 + |b_{mn}|^2 \right) \qquad (29)$$

and the absorption cross section, which is of main interest to us, is obtained from

$$\sigma_a = \sigma_t - \sigma_s. \qquad (30)$$

The criterion for the choice of N,M at which the summations (10)–(13), (27)–(29) are truncated is that the cross sections converge to within a prescribed accuracy.

III. Numerical Calculations

We have applied the point matching method described in Section II to the calculation of the absorption cross section of prolate spheroids of volume equal to that of a man weighing 70 kg. The conductivity and the dielectric constant of the spheroid material were taken to be those of biological tissues with high water content, as given by Johnson and Guy [13]. From the absorption cross section σ_a we obtain the average absorbed power per unit volume P using the relation

$$P = \sigma_a(S/V) \qquad (31)$$

where S is the magnitude of the Poynting vector of the incident beam and V is the volume of the spheroid. An incident power density of 1 mW/cm^2 is assumed throughout.

The point matching method works best for small eccentricities. This could be expected, since all the expansions are made in terms of spherical wavefunctions, so that the convergence is better the smaller the deviation from spherical shape. As the eccentricity increases the convergence of the sums becomes slower, and the size of the system of equations has to be increased, which in turn increases the difficulty of obtaining reliable numerical results. We have found the method to be of little practical value for major to minor axis ratio larger than about 1.5. This is smaller than the ratio which would correspond to a man model, yet it is large enough to exhibit the polarization effects which are of interest. The calculated average absorbed power densities for the three polarizations are shown in Figs. 1 and 2 for

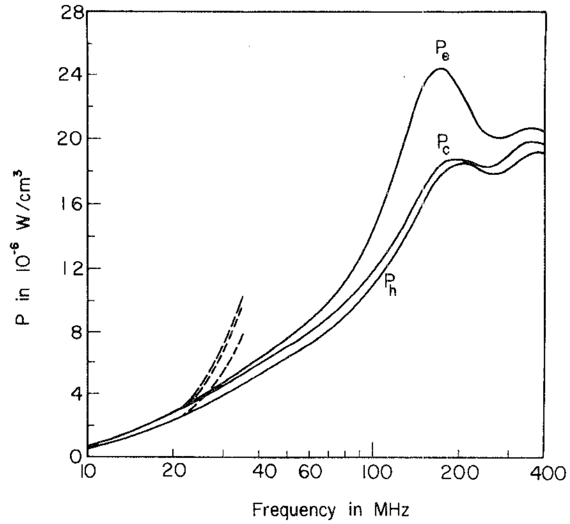

Fig. 1. Frequency dependence of average absorbed power density in a muscle prolate spheroid with $a = 0.297$ m, $a/b = 1.25$, $V = 0.07$ m^3, and incident power density of 1 mW/cm^2. P_e—electric polarization, P_h—magnetic polarization, P_c—cross polarization. The dashed curves show the results obtained from the long wavelength theory.

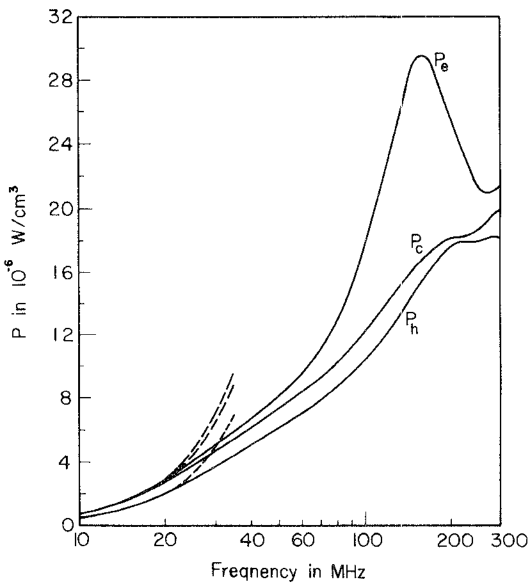

Fig. 2. Frequency dependence of average absorbed power density in a muscle prolate spheroid with $a = 0.335$ m, $a/b = 1.5$, $V = 0.07$ m^3, and incident power density of 1 mW/cm^2. P_e—electric polarization, P_h—magnetic polarization, P_c—cross polarization. The dashed curves show the results obtained from the long wavelength theory.

major to minor axis ratio of 1.25 and 1.5, respectively. The high-frequency cutoff of the calculations was again dictated by the convergence becoming too slow. The cutoff is lower for the larger eccentricity. The frequency range covered by the calculation does, however, extend into the resonance region and the important polarization effects in this region are clearly seen. For comparison we have also shown in Figs. 1 and 2 the absorption calculated from the long wavelength theory employed by Durney *et al.* [7]. According to the expressions used by them, the average absorbed power density for the three polarizations is given by

$$P_h = \tfrac{1}{2}\sigma k_0^2 V((B/\sigma\eta_0)^2 + b^2/10) \tag{32}$$

$$P_e = \tfrac{1}{2}\sigma k_0^2 V((B'/\sigma\eta_0)^2 + a^2b^2/5(a^2 + b^2)) \tag{33}$$

$$P_c = \tfrac{1}{2}\sigma k_0^2 V((B/\sigma\eta_0)^2 + a^2b^2/5(a^2 + b^2)) \tag{34}$$

where

$$B = \frac{1}{u^2 - 1}\left(\frac{u^2}{u^2 - 1} - \frac{u}{2}\ln\frac{u+1}{u-1}\right)^{-1} \tag{35}$$

$$B' = \frac{1}{u^2 - 1}\left(\frac{u}{2}\ln\frac{u+1}{u-1} - 1\right)^{-1} \tag{36}$$

$$u = \frac{a}{(a^2 - b^2)^{1/2}}. \tag{37}$$

From Figs. 1 and 2 it can be seen that the long wavelength method is reliable only for frequencies lower than about 20 MHz.

IV. Discussion and Conclusions

We have found that the point matching method enables the calculation of the absorption in tissue spheroids of moderate eccentricities and over a frequency region which extends into the resonance region, up to $k_0L \simeq 4$, where $L = 2a$ is the long dimension of the spheroid. To our knowledge, this is the first calculation in which the prominent resonance for the electric polarization, shown in Figs. 1 and 2, has been obtained. Qualitatively similar curves have been previously given by Gandhi [4]–[6] and were based on measurements performed on rats, mice and biological-phantom prolate spheroidal bodies. Gandhi has concluded that the absorption at resonance for the electric polarization is larger by a factor of about 10 than for the other two polarizations. If we extrapolate our results for the region $a/b \leq 1.5$ to $a/b \sim 5$–6, as in Gandhi's experiments, we also obtain an order of magnitude difference between the electric polarization and the other polarizations. As to the position of the strongest resonance, Gandhi [6] has estimated it to be at $k_0 L \simeq 1.0$ to 1.6, whereas in our calculations it is found to occur at $k_0L \simeq 1.1$. Gandhi has also concluded that the absorption in the case of cross polarization is only slightly higher than for the magnetic polarization, in agreement with our results. Our curves indicate the existence of secondary absorption maxima at higher frequencies, although the information we can extract about these is rather limited, because of the high-frequency cutoff of the calculation. The experimental data of Gandhi [4] also exhibit secondary resonances.

Finally, we note that we have also performed calculations of the spatial distribution of the absorbed power. We have found that for the spheroids discussed in this work the maximum occurs at the leading surface. This could be expected from the analogous situation for spheres, where internal hot spots do not occur for spheres of radius 10 cm, or larger [1].

References

[1] H. N. Kritikos and H. P. Schwan, "Hot spots generated in conducting spheres by electromagnetic waves and biological implications," *IEEE Trans. Bio-Med. Eng.*, vol. BME-19, pp. 53–58, Jan. 1972.

[2] J. C. Lin, A. W. Guy, and C. C. Johnson, "Power deposition in a spherical model of man exposed to 1–20 MHz electromagnetic fields," *IEEE Trans. Microwave Theory Tech.*, vol. MTT-21, pp. 791–797, Dec. 1973.

[3] H. N. Kritikos and H. P. Schwan, "The distribution of heating potential inside lossy spheres," *IEEE Trans. Bio-Med. Eng.*, vol. BME-22, pp. 457–463, Nov. 1975.

[4] O. P. Gandhi, "Polarization and frequency effects on whole animal absorption of RF energy," *Proc. IEEE* (Lett.), vol. 62, pp. 1171–1175, Aug. 1974.

[5] ——, "Strong dependence of whole animal absorption on polarization and frequency of radio-frequency energy," *Ann. N.Y. Acad. Sci.*, vol. 247, pp. 532–538, Feb. 1975.

[6] ——, "Conditions of strongest electromagnetic power deposition in man and animals," *IEEE Trans. Microwave Theory Tech.*, vol. MTT-23, pp. 1021–1029, Dec. 1975.

[7] C. H. Durney, C. C. Johnson, and H. Massoudi, "Long wavelength analysis of plane wave irradiation of a prolate spheroid model of man," *IEEE Trans. Microwave Theory Tech.*, vol. MTT-23, pp. 246–253, Feb. 1975.

[8] C. C. Johnson, C. H. Durney, and H. Massoudi, "Long wavelength electromagnetic power absorption in prolate spheroidal models of man and animals," *IEEE Trans. Microwave Theory Tech.*, vol. MTT-23, pp. 739–747, Sept. 1975.

[9] M. Kerker, *The Scattering of Light and Other Electromagnetic Radiation*. New York: Academic Press, 1969.

[10] T. Oguchi, "Attenuation and phase rotation of radio waves due to rain," *Radio Sci.*, vol. 8, pp. 31–38, Jan. 1973.

[11] J. A. Morrison and M. J. Cross, "Scattering of a plane electromagnetic wave by axisymmetric raindrops," *Bell Syst. Tech. J.*, vol. 53, pp. 955–1019, July–Aug. 1974.

[12] P. M. Morse and H. Feshbach, *Methods of Theoretical Physics*. New York: McGraw-Hill, 1953.

[13] C. C. Johnson and A. W. Guy, "Nonionizing electromagnetic wave effects in biological materials and systems," *Proc. IEEE*, vol. 60, pp. 692–718, June 1972.